

# SIMULATION OF RIME ICING AND ITS EFFECTS ON AERODYNAMIC CHARACTERISTICS OF AN AIRFOIL

Janusz Sznajder

*Institute of Aviation, Department of Aerodynamics  
Krakowska Av. 110/114, 02-256 Warsaw, Poland  
tel.: +48 22 8460011 ext. 492, fax: +48 22 8464432  
e-mail: janusz.sznajder@ilot.edu.pl*

## **Abstract**

*A mathematical model for simulation of icing dedicated to simulation of ice accretion and its effects on aircraft aerodynamic characteristics in conditions of rime icing is presented. Pure rime icing occurs at lower temperatures than glaze icing and results in higher roughness of the surface of deposited ice. The model accounts for increased surface roughness, in terms of equivalent sand grain roughness, caused by deposited rime ice, which influences generation and dispersion of heat in the boundary layer. Increase of surface roughness is determined by analytical models created upon experimental data obtained in icing wind tunnels. Increased generation of heat is a result of increased tangential stress on the surface and is quantified in the temperature recovery factor determined numerically by a CFD solver. Effects of surface roughness on the intensity of forced convection are quantified by application of Colburn analogy between heat and momentum transfer in the boundary layer, which allows assessment of heat transfer coefficient for known friction coefficient, determined by CFD. The computational method includes determination of the surface distribution of mass of captured water in icing conditions. The model of freezing of captured water accounts for generation of heat due to latent heat of captured water droplets, temperature recovery in boundary layer and kinetic energy of captured droplets. The sinks of heat include forced convection, heating of super cooled droplets, conduction of heat through the ice layer and sublimation. The mathematical model is implemented as user-defined function module in ANSYS Fluent solver. The results include effects of deposited ice, including increased surface roughness on aerodynamic characteristics of an airfoil.*

**Keywords:** *computational fluid dynamics, aerodynamics, two-phase flow, simulations of ice accretion, heat exchange, aircraft engineering, transport, vehicles*

## **1. Introduction**

Accretion of ice deposit on aircraft surface affects its performance in various ways, depending on location, shape and structure of ice deposit, subject to ambient conditions. Particularly vulnerable are leading edges, engine inlets and sensor inlets. Especially harmful for the aerodynamic characteristics is glaze icing occurring when some of the captured water does not freeze immediately on impact but freezes in water-film flow dramatically distorting airfoil contour. A little less harmful is rime icing, occurring usually at lower temperatures and at lower dispersed water content in atmosphere than glaze icing, when droplets freeze immediately upon impact. Experiments in icing wind tunnels, e.g. presented in [1] have shown, that distortion of airfoil contour in rime icing is milder than in glaze icing and the deterioration of lift curve, particularly reduction of maximum lift value, important at take-off and landing conditions may be less severe. However, even without strong distortion of airfoil contour, increase of surface roughness due to deposited ice is present in rime icing and its effects on aircraft aerodynamic characteristics, particularly on drag require study.

## **2. Accounting for surface roughness**

Models relating surface roughness caused by deposited ice to ambient atmospheric conditions were proposed by Shin and Bond [1]. The model (one of two proposed) applied in the present

work accounts for Median Volume Diameter (MVD), Liquid Water Content (LWC), ambient temperature (T) and airfoil chord (c). The result is height of equivalent surface roughness, which is height of uniform sand grains investigated by Nikuradse [3]. This approach to modelling the effects of roughness, making use of results obtained by Nikuradse is widely applied in engineering applications and allows relating effects of different types of roughness to effects of uniform sand grains investigated systematically over wide range of Reynolds numbers. One should remember, however, that the height of equivalent roughness might differ from the real height of investigated roughness elements, shape of which differs from uniform sand grains. This approach, taking equivalent roughness height as input to analysis of boundary layer flow is implemented in CFD solvers, also in ANSYS Fluent CFD solver used in the present work. Surface roughness caused by growing ice deposit has strong effects not only on aerodynamic characteristics (increase of drag), but influences also emission and dispersion of heat on ice-air contact zone.

Accounting for surface roughness in Computational Fluid Dynamics requires modelling its effects on velocity distribution near rough walls in order to avoid the necessity of resolving shape of individual roughness elements in computational grid. Modelling effects of surface roughness is based on observation that wall roughness changes relation between nondimensional quantities  $y^+$  and  $u^+$  in the logarithmic region of boundary layer by modification of additive constant B in relation [2]:

$$u^+ = \frac{1}{k} \ln(y^+) + B, \quad (1)$$

moving the curve downwards, towards lower values of  $u^+$ .

In ANSYS Fluent [4] this relation has slightly different form:

$$\frac{uu^*}{\tau_w/\rho} = \frac{1}{k} \ln \left( E \frac{\rho u^* y}{\mu} \right) - \Delta B, \quad (2)$$

where  $\Delta B$  is dependent on nondimensionalised surface roughness height  $K_s^+$ ,  $K_s^+ = \rho K_s u^*/\mu$ .

For fully rough conditions, when  $K_s^+ > 90$ ,

$$\Delta B = (1/k) \ln(1 + C_s K_s^+). \quad (3)$$

The downward shift of the  $u^+ = f(y^+, K_s^+)$  curve due to  $\Delta B$  leads to singularity in  $u^+$  for low values of  $y^+$ . In order to avoid the singularity, different strategies are adopted for different turbulence models. For Spalart-Almaras model the value of  $K_s^+$  is reduced for low values of  $y^+$  according to formula:  $K_s^+ = \min(K_s^+, y^+)$ . This avoids the singularity, but requires preparation of grids with large enough height of first layer of cells, in order to avoid reduction of  $K_s^+$ . This may lead to first layer heights producing  $y^+$  values higher than recommended for the Spalart-Almaras turbulence model. The other approach, adopted in turbulence models based on  $\omega$  equation and in some models based on the  $\varepsilon$  equation consists in increasing first cell  $y^+$  value,  $y^+ = y^+ + K_s^+/2$ . This may be interpreted as shifting the wall upwards, to 50% of roughness height, which physically is consistent with blockage effect of surface roughness. In the present work the values of roughness presented in Fig. 1 result in  $K_s^+$  values higher than 150, which would require first cell heights producing similar value of  $y^+$ , far above height recommended in the practice of CFD simulations. For this reason, the  $k-\omega$  model was chosen for numerical analyses. Additional step in turbulence modelling consisted in calibration of the  $C_s$  constant in equation (3). Its default value of 0.5 was chosen by the Fluent software developers to reproduce Nikuradse resistance data in pipes. In the present case of flow over airfoil the value of 0.35 was chosen, which reproduced velocity profile in boundary layer, presented by Nikuradse in [3], which is shown in Fig. 2. The comparison was conducted at location beyond high-pressure gradients, where  $y^+$  parameter was almost constant along airfoil surface. It must be noted, that velocity profile, nondimensionalised and plotted against  $\log y/K_s$  is independent of the height of surface roughness [3].

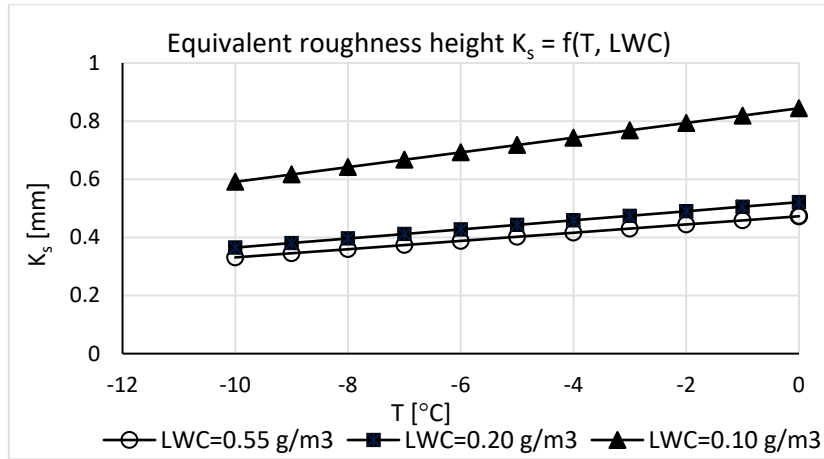


Fig. 1. Equivalent roughness height of surface covered with rime ice vs ambient temperature [1]

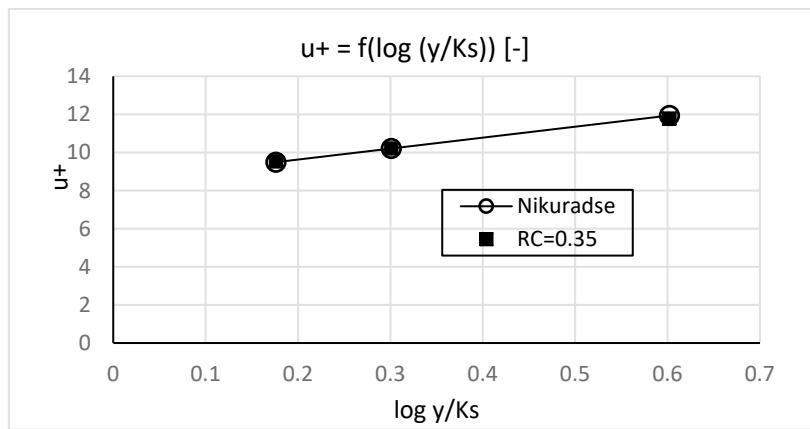


Fig. 2. Comparison of nondimensionalised velocity  $u^+$  vs. nondimensionalised distance from surface obtained with present method in Fluent solver and of results of Nikuradse presented in [3]

### 3. Heat exchange in ice-air interface

The model of production and dispersion of heat in the ice-air contact zone used in present work is the one proposed by Myers [5]. It consists of:

a) terms describing energy transported into air-water-ice contact zone:

$$Q_k = (\beta \rho_{d \text{ inf}} V_{\text{inf}}) \frac{V_{\text{inf}}^2}{2} - \text{kinetic energy of water droplets,} \quad (4)$$

$$Q_l = L_f \dot{m}_{\text{ice}} - \text{latent heat of freezing,} \quad (5)$$

$$Q_{aw} = r \cdot \frac{H_{aw} V_{\text{inf}}^2}{2c_a} - \text{heat released in the boundary layer,} \quad (6)$$

where  $r$  is a temperature recovery factor,  $r = \frac{T - T_{\infty}}{T_{\text{tot}} - T_{\infty}}$ ,

b) terms describing energy transported away from the contact zone:

$$Q_{ci} = h(T_i - T_a) - \text{convection over ice layer,} \quad (7)$$

$$Q_s = \chi_s e_0 (T_i - T_a) = q_s (T_w - T_a) - \text{sublimation heat,} \quad (8)$$

$$Q_d = \beta \rho_{d \text{ inf}} V_{\text{inf}} (T_w - T_a) = q_d (T_w - T_a) - \text{warming of supercooled droplets,} \quad (9)$$

$$Q_{\text{cond}} = \kappa_i \frac{T_f - T_s}{B} - \text{conduction of heat through ice to substrate,} \quad (10)$$

where  $h$  is convection coefficient,  $\beta$  is water collection efficiency,  $\beta = \frac{\rho_d \vec{V}_d \cdot \vec{n}}{\rho_{d \text{ inf}} \vec{V}_{\text{inf}}}$ , and is computed in simulations of two-phase flow over the airfoil. It is positive on portions of surface hit by dispersed water, conf [6].

Determination of type of ice accretion (rime or glaze) is conducted according to [5], by calculating ice thickness when water first appears. It is given by:

$$B_g = \frac{\kappa_i(T_f - T_s)}{\beta \rho_{d \text{ inf}} V_{\text{inf}} L_f + [Q_a + Q_k - (q_c + q_d + q_e)(T_f - T_a)]} \quad (11)$$

A case of a negative denominator of Eq. 11 over entire airfoil corresponds to conditions when too little heat is produced in the ice-air interface for sustaining liquid water and only rime ice is produced.

One of sources of heat in the boundary layer is aerodynamic heating, described by recovery factor. The well-known definition of temperature recovery factor  $r$  is:

$$r = \frac{T - T_\infty}{T_{\text{tot}} - T_\infty}, \quad (12)$$

where  $T$  is local temperature at surface point,  $T_{\text{tot}}$  and  $T_\infty$  are total and static free-stream temperatures. As it can be seen in equation (12), the factor  $r$ , dependent on local static temperature is a function of surface coordinates. Temperature recovery factor may be determined experimentally or computationally based on equation (12), assuming adiabatic boundary conditions on the surface. Fig. 3 presents surface distribution of temperature recovery factor computed for NACA 0012 airfoil at angle of attack  $\alpha$  of  $0^\circ$ ,  $Re = 4.2$  million,  $M = 0.21$ , compared with widely used approximate formula for turbulent boundary layer, dependent on Prandtl number and with constant value given in [5]. Computations were conducted for rough surface, with  $K_s$  equal to  $0.56 \text{ mm}$  and for smooth surface. It can be seen that the computed values of  $r$  change from unity in the stagnation point to values lower than constant-value approximations, and, that surface roughness increases recovery factor over smooth-surface values.

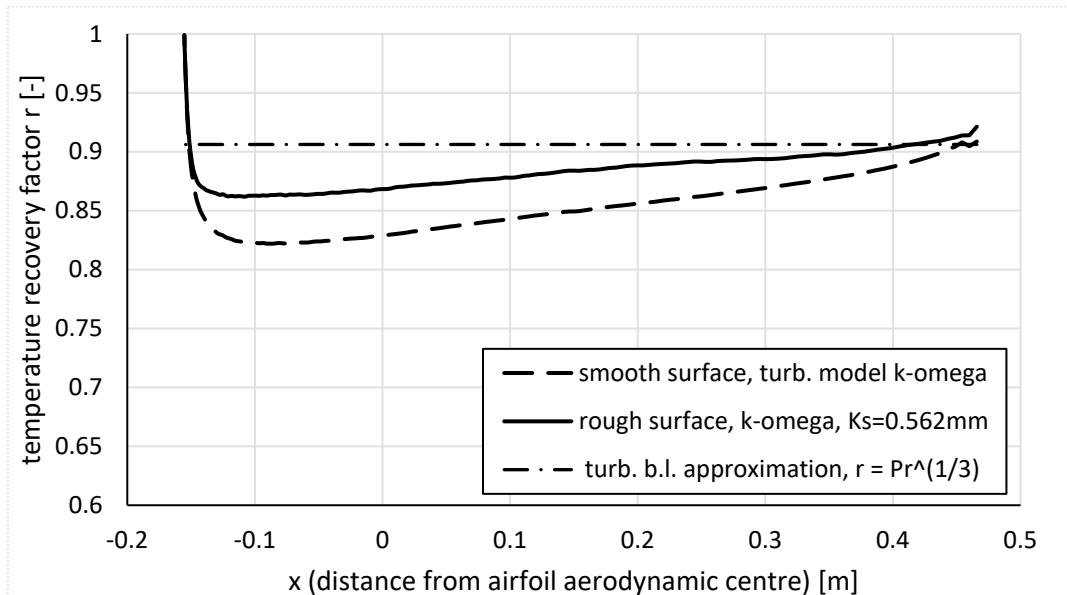


Fig. 3. Dependence of temperature recovery factor on surface roughness and location along airfoil chord

Significant amount of heat generated during ice accretion is released by forced convection. This heat may be estimated based on analogy between momentum transfer and heat transfer in boundary layer. The well-known Reynolds analogy, based on observation that the same

mechanisms are responsible for these phenomena provides relation between heat transfer coefficient, friction coefficient and free-stream velocity:

$$\frac{f}{2} = \frac{h}{\rho C_p V}. \quad (13)$$

Its extension, the well-known Colburn analogy, introduces influence of Prandtl number:

$$\frac{f}{2} = \frac{h}{\rho C_p V} Pr^{2/3}. \quad (14)$$

Similarly to recovery factor, heat transfer coefficient obtained from (13) or (14) is a function of surface coordinates, due to dependence on local friction coefficient. The values of heat transfer coefficients, obtained based on Reynolds analogy and Colburn analogy in the same conditions as in the case of temperature recovery factor are shown in Fig 4. These values are compared with constant value given in [5].

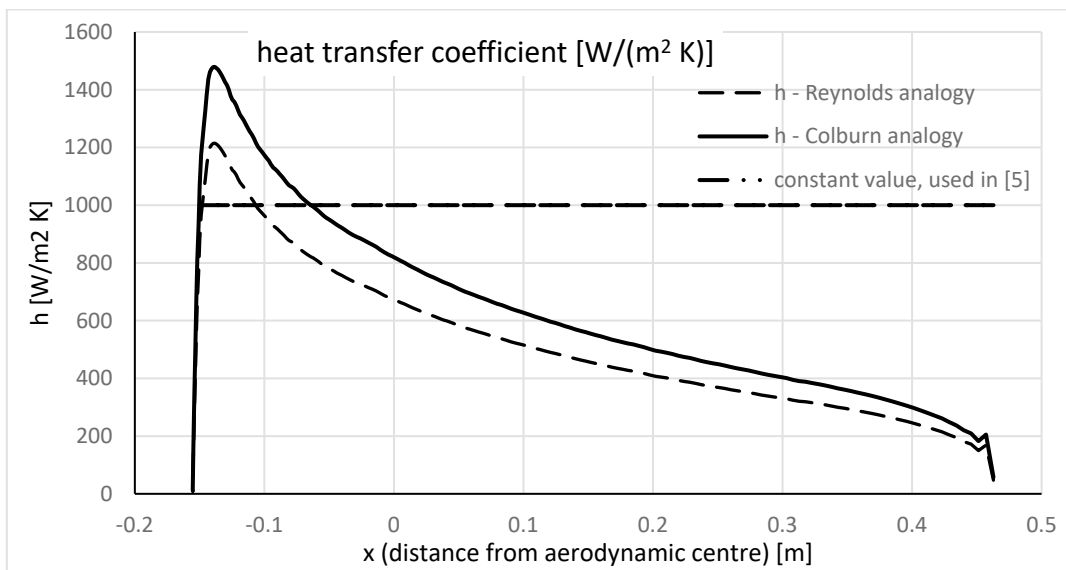


Fig. 4. Surface distribution of heat transfer coefficient calculated for NACA 0012 airfoil applying Reynolds and Colburn analogies

#### 4. Simulation of rime ice accretion and its effects on aerodynamic characteristics of NACA 0012 airfoil

Computational model of ice accretion with terms describing heat exchange on the surface exposed to icing condition given by Equations (4-10) was applied for simulation of two-phase (air and dispersed, supercooled water) flow over NACA 0012 airfoil. The simulated flow conditions were similar to conditions in icing wind-tunnel experiment described in [1]. The total temperature was  $-26.11^{\circ}\text{C}$  ( $-15^{\circ}\text{F}$ ), Mach number 0.21, angle of attack  $\alpha = 4^{\circ}$ ,  $Re = 4.2$  million. The supercooled liquid water content (LWC) was  $1 \text{ g/m}^3$ , median-volume diameter of water droplets was  $20 \mu\text{m}$ .

Determination of distribution of captured water on airfoil surface was done with Eulerian method described in [6]. Analysis of heat production and dispersion terms according to Eq. (11) indicated rime icing. In these conditions, ice growth is determined entirely by the distribution of mass of captured water. The simulation re-created a 360s-long ice accretion experiment. The icing time was divided into 6 60s-long intervals. At the beginning of each of the intervals, the surface distribution of captured water mass was determined, and during each interval the equation of ice accretion was integrated in time with algorithm described in [7], assuming unchanged distribution of captured water during one interval. The final shape of rime-ice deformation of airfoil contour is shown in Fig. 5. It is very close to experimental and simulation results presented in [1].

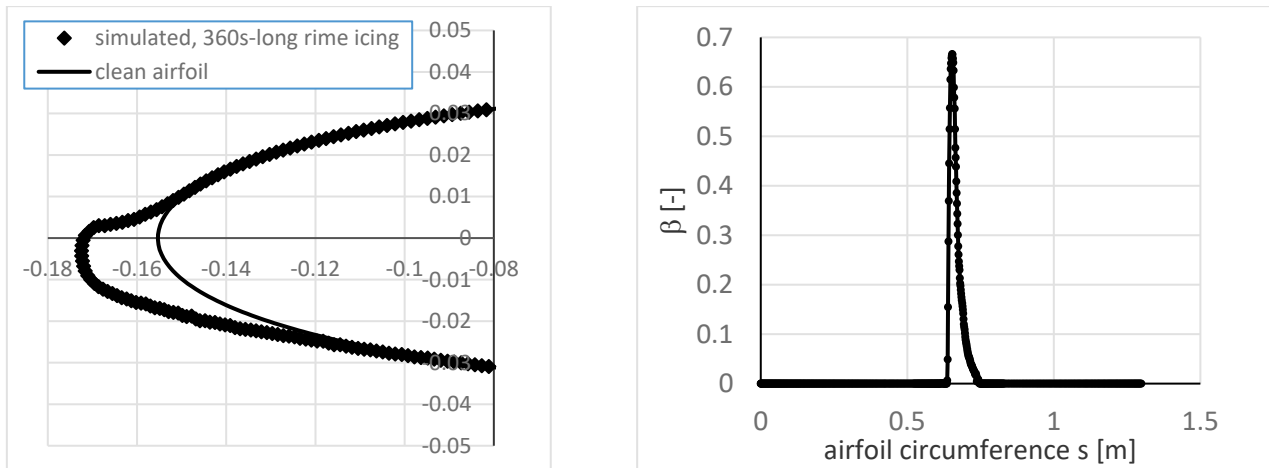


Fig. 5. Comparison of clean-airfoil contour and contour of airfoil deformed by rime ice after simulated 360-s long ice accretion (left) and distribution of coefficient of water collection efficiency  $\beta$  in the final accretion stage (right)

Rime icing is known for increasing roughness of the base surface, which affects mostly drag force. Flow simulations should account for increased surface roughness on the portions of surface affected by icing. In the presented flow simulations, three options of increasing surface roughness were tested: 1). The equivalent roughness height was increased over the portion of circumference with non-zero  $\beta$  coefficient (area bounded by dashed line in Fig. 6, for which value of flag variable was set to 1). As it can be seen, it is a sub-portion of a larger area, for which the free-stream velocity has negative component in the direction normal to airfoil surface. 2) The equivalent roughness height was increased in this larger area, oriented towards free stream, bounded by continuous line. 3) Equivalent roughness height was increased over the entire airfoil circumference. In each case the equivalent roughness height, described in Paragraph 1 was increased to the same value of 0.35 mm, following formulas described in [1] and depicted in Fig. 1. The results of drag computations are presented in Tab. 1. Values of drag and lift coefficient obtained for undeformed, smooth airfoil were  $C_d = 0.0104$  and  $C_l = 0.4497$ .

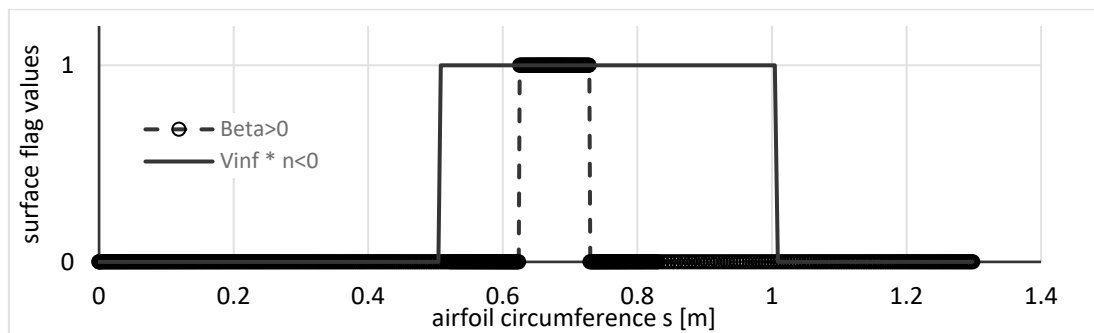


Fig. 6. Visualisation of airfoil circumference fragment with non-zero predicted water collection efficiency  $\beta$ , and of portion of circumference directed towards free-stream velocity (flags set to 1)

Tab. 1. Comparison of experimental and computed values of drag and lift coefficients in icing conditions analysed in the article

	Airfoil deformed, smooth surface ( $K_s=0$ )	Case (1)	Case (2)	Case (3)	Experiment [1]	Numerical method [1]
$C_d$	0.01190	0.013007	0.016879	0.021198	0.0233	0.0202
$\Delta\% C_d$ w.r.t. experiment	-48.93	-44.18	-27.55	-9.02		-13.30
$C_l$	0.4403	0.4395	0.4322	0.4189	not available	not available

The present solution of airflow was obtained with solution of URANS equations and  $k-\omega$  turbulence model of ANSYS-Fluent v.18 with surface roughness set using a DEFINE\_PROFILE macro in a user-defined function. It can be seen, that increase of surface roughness height solely on the surface fragment with positive water collection efficiency, and even on the larger portion, directed towards free-stream led to underestimated value of drag coefficient. The closest-to-experiment value was obtained with surface roughness height increased over the entire airfoil circumference. Similar results were obtained by authors of work [1], which used the 2D LEWICE/IBL code, also with simulated roughness increased over the entire airfoil. In work [1], a different method for calculating distribution of collection efficiency  $\beta$  was used. Authors of work [1] used particle-tracking method, whereas in present work a solution of dispersed water phase treated as continuous phase was obtained using a finite-volume algorithm. In work [1], the airflow solution was obtained using panel method with coupled turbulence model using modified mixing length and wall-damping expression of the Cebeci-Smith model. The application of viscous flow simulations in the present method allows for insight into the structure of computed drag force, which in case 3), closest to experiment are 64% viscous and 36% pressure force. This underscores the need of adequate modelling of surface roughness in simulation of surface icing.

## 5. Conclusions

1. Adequate modelling of effects of surface roughness due to rime icing required increasing simulated roughness height over the entire airfoil, not only over area with positive water collection coefficient. This may be due to simplifications in the modelling of two-phase flow – representing dispersed phase with one diameter of droplets, neglecting secondary effects as droplet breakup, and splashing on impact. It also indicates need of further experimental research on icing.
2. Increase of drag due to rime icing is roughly 100% value of drag of clean surface. This may be an important issue in operating of aircraft. Maintaining force balance in landing approach in icing conditions, with reduced power, may require different throttle settings than in good weather, particularly with de-icing systems having passive phases, e.g. pneumatic boots.
3. High increase of drag due to rime icing may be particularly dangerous for unmanned aircraft or drones with low available power.

## References

- [1] Shin, J., Bond, T. H., *Experimental and computational ice shapes and resulting drag increase for a NACA 0012 airfoil*, NASA Technical Memorandum 105743, 1992
- [2] Versteeg, H. K., Malalasekera, W., *An introduction to computational fluid dynamics*, Pearson Education Limited, 1995, 2007.
- [3] Nikuradse, J., *Laws of flow in rough pipes*, National Advisory Committee for Aeronautics, Technical Memorandum 1292, 1950.
- [4] *ANSYS Documentation*, available with software and online at <https://ansyshelp.ansys.com>, ANSYS, v.18.
- [5] Myers, T., Extension to the Messinger model for aircraft icing, *AIAA Journal*, Vol. 39, No. 2, 2001.
- [6] Sznajder, J., *Determination of water collection on two- and three-dimensional aerodynamic surfaces in external two-phase flow in atmospheric conditions*, *Journal of KONES Powertrain and Transport*, Vol. 23, No. 1, pp. 369-376, 2016.
- [7] Sznajder, J., Sieradzki, A., Stalewski, W., *Determination of ice deposit shape and ice accretion rate on airfoil in atmospheric icing conditions and its effects on airfoil characteristics*, *Journal of KONES Powertrain and Transport*, Vol. 24, No. 2, pp. 271-278, 2017.

*Manuscript received 25 May 2018; approved for printing 30 August 2018*

